View Article Online / Journal Homepage / Table of Contents for this issue

Synthesis of gold nanoparticles inside polyelectrolyte brushes

Omar Azzaroni,[a] Andrew A. Brown,[a] Nan Cheng,[a] Alexander Wei,[b] Alain M. Jonas[c] and Wilhelm T. S. Huck*[ad]

Received 2nd April 2007, Accepted 31st May 2007
First published as an Advance Article on the web 12th June 2007
DOI: 10.1039/b704849a

Published on 12 June 2007. Downloaded by Michigan State University on 16/01/2016 02:00:57.

In this work we report on the synthesis and characterization of Au nanoparticles grown in the inner environment of cationic polyelectrolyte brushes. The nanocomposite synthesis relies on loading the macromolecular film with $AuCl_4^-$ precursor ions followed by their *in situ* reduction to Au nanoparticles. We observed that the nanoparticles are uniform in size and are fully stabilized by the surrounding polyelectrolyte chains. Moreover, XRR analysis revealed that the Au NPs are formed within the polymer-brush layer. AFM experiments confirmed that the swelling behaviour of the brush layer is not perturbed by the presence of the loaded NPs. The Au NP-poly-METAC nanocomposite is remarkably stable to aqueous environments, suggesting the feasibility of using this kind of nanocomposite systems as robust and reliable stimuli-responsive platforms.

Introduction

The synthesis and characterization of metal nanoparticles (NPs) embedded in supporting matrices has become an extremely active research field in recent years.[1–3] Potential applications of such nanocomposites include the development of materials with new or unusual optical properties or catalytic activities, or nanocomposites with novel mechanical function.[4–6] More interesting opportunities arise when the polymer matrix responds to external stimuli such as pH, solvent polarity, and ion-selective adsorption.[7–9] One successful approach for making nanocomposites relies on loading the polymer matrix with metal-ion precursors and synthesizing the NPs *in situ*. In many cases, the final step involves hydrogenation or the use of reductants like $NaBH_4$ in aqueous solution.[10] Here the macromolecular matrix has a dual role: to provide a scaffold for immobilizing NPs and preventing aggregation, and to serve as a capping agent for limiting NP growth. Charged polymers (polyelectrolytes) are especially useful matrices for preparing nanocomposites; examples include NPs synthesized and encapsulated within dendrimers,[11] and polyelectrolyte multilayers[12–14] or brushes[15] on solid supports. All of these involve the coordination of ionic precursors, followed by their *in situ* reduction to NPs with an appropriate agent.

Despite the growing popularity of polyelectrolytes for preparing nanocomposite films, questions remain regarding how the nanoscale architecture of the polyelectrolyte layer affects the nucleation, growth and distribution of NPs within the composite, and how the embedded NPs affect the swelling properties of the polyelectrolytes. In this paper we investigate some of these fundamental issues by preparing and characterizing nanocomposites comprised of gold NPs within cationic polyelectrolyte brushes of controlled thickness. The *in situ* reduction of gold chloride within these polymer brushes produces a homogeneous distribution of well-segregated Au NPs with minimal aggregate formation. We show that the Au nanoparticles do not affect the swelling properties of the ultrathin polyelectrolyte layer, and evaluate the extent to which changes in nanocomposite ultrastructure can be correlated to changes in optical absorption. With regard to the latter, we note that Minko *et al.* have recently demonstrated the use of NP-embedded polyelectrolyte brushes on Au substrates as a reagent-free sensor of chemical sorption.[9]

[a]*Melville Laboratory for Polymer Synthesis, University of Cambridge, Lensfield Rd., Cambridge, UK CB2 1 EW*
[b]*Department of Chemistry, Purdue University, 560 Oval Drive, West Lafayette, IN 47907, USA*
[c]*Unité de Chimie et de Physique des Hauts Polymères, Université catholique de Louvain Place Croix du Sud, B1348 Louvain-la-Neuve, Belgium*
[d]*The Nanoscience Centre, University of Cambridge, UK*

Experimental

Substrate preparation

Patterned gold samples were prepared by microcontact printing (μCP) of a thiol initiator (ω-mercaptoundecylbromobutyrate) onto clean gold-coated substrates, prepared by the controlled evaporation of 14 nm Cr and 100 nm Au on a silicon wafer. For brushes grown on glass or Si/SiO_2, 2-bromoisobutyric acid-3′-(trichlorosilyl)propyl ester was used to prepare the initiator-modified substrates using previously reported conditions.[16] In a typical experiment, a plasma oxidized silicon wafer is placed in a crystallizing dish and covered with a filtered (0.22 μm pore filter) solution of trichlorosilane initiator (10 μL) in dry toluene (30 cm^3), followed by dry triethylamine (Et_3N) (50 μL). The dish is covered, sealed, and left at room temperature for 18 h. The wafer is washed with toluene, sonicated in toluene for 1 min, washed with acetone then absolute ethanol, and dried under a stream of N_2.

Polyelectrolyte-brush formation

All chemicals were used as received. A 75% aqueous solution of 2-(methacryloyloxy)ethyltrimethylammonium chloride (METAC, 40 mmol) was diluted 1 : 1 with 80% aqueous

View Article Online

Published on 12 June 2007. Downloaded by Michigan State University on 16/01/2016 02:00:57.

methanol (10 mL) at 20 °C, and degassed for 15 min by passing a continuous stream of dry N_2 through the solution with stirring. To this solution was added 2,2′-dipyridyl (416 mg, 2.7 mmol), Cu(I)Cl (105 mg, 1.1 mmol) and Cu(II)Cl_2 (14 mg, 0.11 mmol). The mixture was then stirred and degassed with a stream of dry N_2 for another 15 min. Initiator-coated wafer samples ($\sim$1 cm^2 each) were sealed in Schlenk tubes, degassed (4 × high-vacuum pump–N_2 refill cycles), and kept at 20 °C under N_2. The polymerization solution was then syringed into each Schlenk tube, adding enough solution to submerge each sample completely. After various polymerization times the samples were removed, washed with water then methanol, and dried under a stream of N_2.[17]

Auger electron spectroscopy

Surface elemental analyses with AES (INIFTA – La Plata) were carried out using a single-pass cylindrical mirror analyzer (CMA, Physical Electronics). All spectra were recorded in differential mode ($dN(E)/dE$) with multipoint analysis across each sample to obtain an average estimate of surface composition.

Atomic force microscopy

AFM experiments were carried out in a liquid cell using a MacMode PicoSPM magnetically driven dynamic force microscope (Molecular Imaging). Images were taken using commercially available type II MAClevers with a nominal force constant of 2.8 N m^{-1} at a driving frequency of 19 Hz in the liquid environment.

Transmission electron microscopy

TEM samples were prepared from polyelectrolyte-NP layers on glass by first scraping the dry substrate with a razor edge. A glass cover slip was placed over the abraded substrate with a drop of deionized water, which was then briefly sonicated to disperse the detached polyelectrolyte-NP composite. A drop of this solution was deposited and dried on a carbon-coated 200-mesh Cu grid (Agar Scientific). Images were obtained using a JEOL 200CX transmission electron microscope using an accelerating voltage of 100 kV.

X-Ray reflectivity

XRR was measured with a 2-circle goniometer (Siemens D5000) with a 30 cm radius and 0.002° positioning accuracy. The incident beam (CuKα radiation, λ = 0.15418 nm) was obtained from a rotating anode (Rigaku, Japan) operated at 40 kV and 300 mA, fitted with a collimating mirror (Osmic, Japan) delivering a parallel beam of about 0.0085° angular divergence. The beam size was defined by a 40 mm-wide slit placed 17.5 cm away from the focal spot. The sample was fixed at the centre of the goniometer by an automated procedure, using a vertical stage of 1 μm resolution. The intensity was scaled to unit incident intensity, and corrected for spill-over at very low angles of incidence. Data are reported as a function of k_{Z0}, the vertical component of the wavevector of the incident photons in a vacuum. The reflectivities were analyzed by fitting the data to an electron-density model consisting of a stack of n slabs of adjustable height, thickness and roughness. Fits were performed starting with n = 1, and progressively increasing the number of slabs n until the simulated reflectivity reproduced the experimental data within an acceptable error limit.

Results and discussion

Cationic polyelectrolyte brushes were prepared from aqueous solutions of 2-(methacryloyloxy)ethyltrimethylammonium chloride (METAC) and were grown on gold, Si and/or glass substrates by surface-initiated atom transfer radical polymerization (ATRP).[18–20] All the details regarding polymer-brush growth were reported in a previous publication.[17] Au NPs were prepared by first saturating the polyelectrolyte-brush layer with gold chloride (Fig. 1). Sorption of $AuCl_4^-$ is driven by the strong affinity of the quaternary ammonium groups (QA^+) for highly polarizable and weakly hydrated anions.[21,22] We have demonstrated that such anions are tenaciously retained by polyelectrolyte-brush layers, with the polymer matrix acting as a nanoreservoir.[23,24]

The ion-exchange process involved in the precursor uptake is described as eqn (1), in which Cl^- anions are efficiently displaced by $AuCl_4^-$ species.

$$(QA^+Cl^-)_{(brush)} + AuCl_4^-{}_{(aq)} \rightarrow [(QA^+)AuCl_4^-)]_{(brush)} + Cl^-{}_{(aq)} \quad (1)$$

It should be noted that the affinity of QA^+ groups for the chloride complexes of transition metal ions is commonly featured in commercial ion-exchange resins for extracting metal salts.[25,26] In effect, the poly-METAC brushes behave as ion-pairing adsorbent layers to preconcentrate the metal precursors in the substrate.

The precursor uptake was carried out by immersing the poly-METAC-modified surfaces in aqueous solutions of $HAuCl_4$ (pH = 1) for 30 minutes. These conditions provided us with a reproducible and linear relationship between the content of $AuCl_4^-$ in the brush layer and its concentration in the aqueous solution. This was demonstrated by measuring the content of adsorbed Au(III) ions in the poly-METAC brushes as a function of concentration by ultraviolet absorption spectroscopy, based on a well-defined charge-transfer band at λ = 318 nm (Fig. 2a).

After loading the precursor gold salts into the polyelectrolyte-brush layer, the substrates were treated with aqueous $NaBH_4$ solution, a widely used method of reducing $AuCl_4^-$ to colloidal gold.[27–29] Borohydride reduction is a very fast process requiring only a few seconds to reduce most of the adsorbed $AuCl_4^-$ species to Au NPs, which produces an increase in absorbance intensity centered at 542 nm, corresponding to the localized plasmon resonance of Au NPs (Fig. 2b). The increase in absorbance intensity was observed to be approximately linear with the loading of $AuCl_4^-$ ions within the polyelectrolyte brushes, indicating an efficient conversion to colloidal Au. The position and linewidths of the plasmon-resonance bands indicate that (i) the nanoparticles are well separated from one another, and (ii) the majority of the Au NPs are at least 5 nm in diameter. Gold

 This journal is © The Royal Society of Chemistry 2007

View Article Online

Published on 12 June 2007. Downloaded by Michigan State University on 16/01/2016 02:00:57.

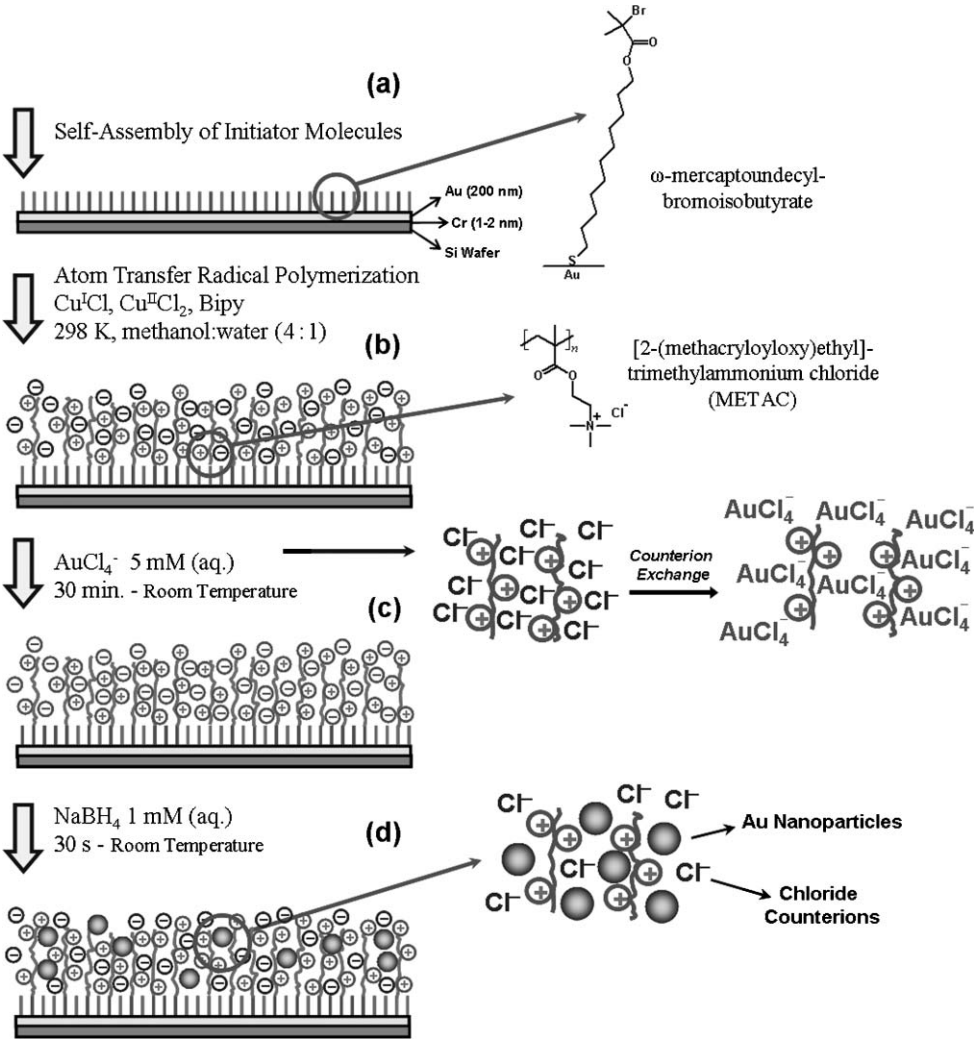

Fig. 1 Schematic outline of the procedure used to synthesize Au nanoparticles inside polyelectrolyte brushes. (a–c) Poly-METAC brushes are synthesized by surface-initiated aqueous ATRP, followed by immersion in $AuCl_4^-$ solution for 30 min. (d) The Au-loaded brushes are then treated with $NaBH_4$ to produce mostly metallic Au NPs, along with some partially reduced Au species.

nanoparticles in close proximity are well known to experience a significant coupling of their plasmon resonances, resulting in a redshift and broadening of their absorbance peak.[30–32] With respect to particle size, the plasmon linewidth is known to increase inversely with NP size due to surface-scattering effects,[30] and becomes noticeably broader for particles smaller than 5 nm.

Auger electron spectroscopy (AES) was performed on the poly-METAC brushes loaded with gold ions, in order to determine the retention of gold within the brush layer after reduction (Fig. 3). Samples soaked in 16 mM $AuCl_4$ solutions were extensively washed with water both before and after reduction; in the latter case, a fourfold decrease in the Cl signal was observed whereas the Au signal remained constant, indicating no significant leaching of Au NPs from the brush. The NPs were presumably passivated by residual Cl ions, and were thus most likely retained within the polyelectrolyte brush by electrostatic interactions. Furthermore, a significant Cl signal remained, suggesting the presence of other ionic Cl species. In particular, we considered that the partial reduction of $AuCl_4$ would result in a significant accumulation of Au(I)Cl or very small Au clusters, whose complete reduction would be retarded by their strong adsorption to the polyelectrolyte brush. Although Au(I)Cl is optically active in the UV region, it is difficult to characterize in the presence of $AuCl_4^-$ ions and Au NPs.

The Au-loaded polyelectrolyte brushes were also characterized by transmission electron microscopy (TEM) by cleaving the poly-METAC layer from the glass substrate, and depositing the dispersed materials onto a carbon-coated Cu grid. Colloidal Au NPs embedded within the brushes were clearly visible, and were well dispersed with an average diameter of 9 nm (Fig. 4). These were surrounded by a dendritic halo corresponding to an encapsulating layer of poly-METAC. The polyelectrolyte capsules were uniform with an average diameter of 60 nm, and the effective thickness of the capsules (*ca.* 25 nm) was in accord with the thickness of the initial poly-METAC layer measured by X-ray reflectivity (see below). Although a few aggregates were observed (Fig. 4b), the majority of Au NPs appeared to have formed as isolated

View Article Online

Published on 12 June 2007. Downloaded by Michigan State University on 16/01/2016 02:00:57.

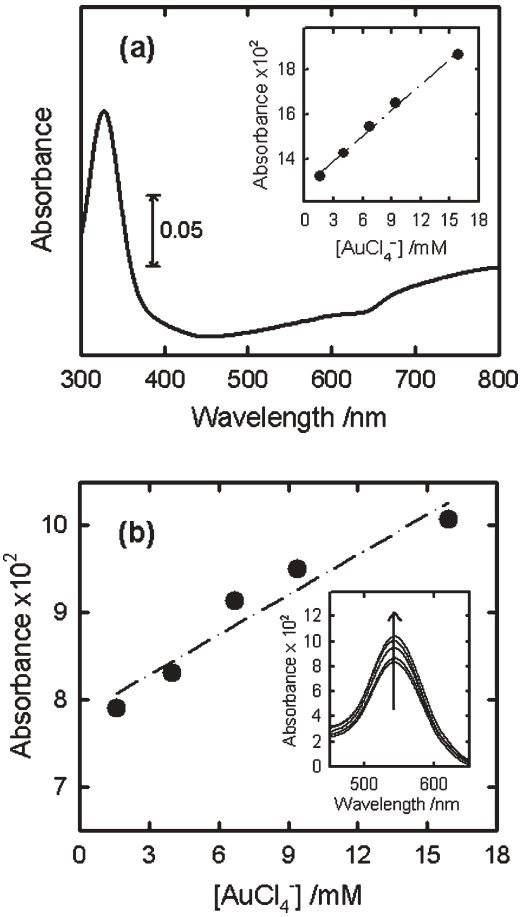

Fig. 2 (a) UV-Visible absorbance spectrum of poly-METAC brushes on a glass substrate, after 30 min immersion in 1.5 mM $HAuCl_4$ solution. Inset shows a linear increase in UV absorbance with $AuCl_4^-$ concentration. (b) Absorbance plot (λ = 542 nm) indicating relative density of Au nanoparticles inside poly-METAC-brush layers after treatment with $NaBH_4$. Inset shows an increase in absorbance intensity with $AuCl_4^-$ sorption, as described in (b). No appreciable shifts in λ_{max} were observed, indicating minimal NP aggregation.

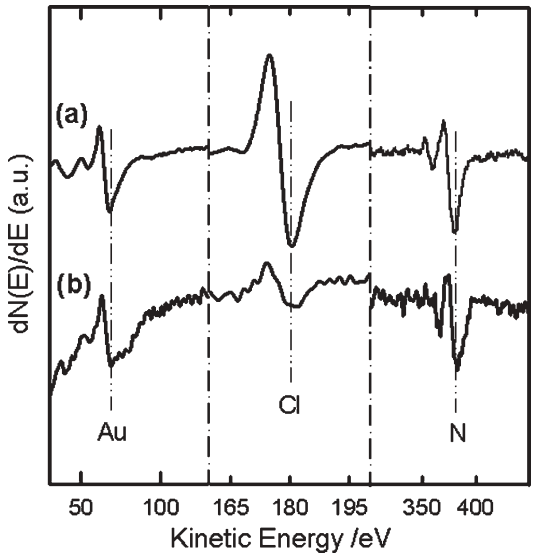

Fig. 3 Auger electron spectroscopy (AES) spectra corresponding to: (a) $AuCl_4^-$-loaded poly-METAC brushes and (b) $AuCl_4^-$-loaded poly-METAC brushes after BH_4^- reduction. In the spectra are detailed the AES signals for Au (NVV, 69 eV), Cl (LVV, 181 eV) and N (KLL, 380 eV).

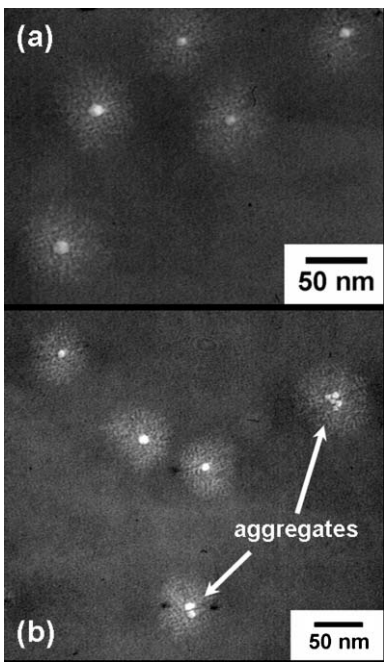

Fig. 4 Transmission electron microscopy (TEM) images corresponding to Au NPs (9 ± 1 nm) synthesized inside the poly-METAC brush. (a) The TEM images suggest that most of Au NPs exist as isolated particles, although a few aggregates were also formed. (b) The halo around the NPs can be attributed to the capping of NPs by the polyelectrolyte layer, stained by partially reduced Au species.

particles, commensurate with the illustration in Fig. 1. Notably, the TEM visualization of the polyelectrolyte layer was possible due to the presence of residual Au(I)Cl or very small Au nanoclusters, whose large electron-scattering cross-sections provide useful EM contrast to the polyelectrolyte capsules, similar to other heavy-metal staining agents.

In order to elucidate the influence of the brush architecture on NP growth, we carried out X-ray reflectivity (XRR) measurements of poly-METAC brushes grown on SiO_2/Si prior to and after $AuCl_4$ loading and reduction (Fig. 5a). The X-ray reflectograms exhibit well-defined Kiessig fringes, resulting from interference of the beams reflected by the interfaces of the film; the damping of the fringes upon NPs growth is indicative of increased film roughness. More information could be extracted by fitting the XRR data to an electron-density profile model as a function of distance from the substrate (Fig. 5b). For both samples, the electron-density profiles show first a plateau of about 0.7 electrons per $Å^3$, which is typical of Si. The plateau ends with a small density perturbation resulting from the plasma treatment of Si wafers, and is followed by a rapid decrease corresponding to the Si–film interface. For the brush devoid of NPs, the electron density reaches a second plateau at about 0.38 electrons per $Å^3$ followed by a relatively sharp decrease to zero, corresponding to a homogeneous brush layer between the Si substrate and air.

 This journal is © The Royal Society of Chemistry 2007

View Article Online

Published on 12 June 2007. Downloaded by Michigan State University on 16/01/2016 02:00:57.

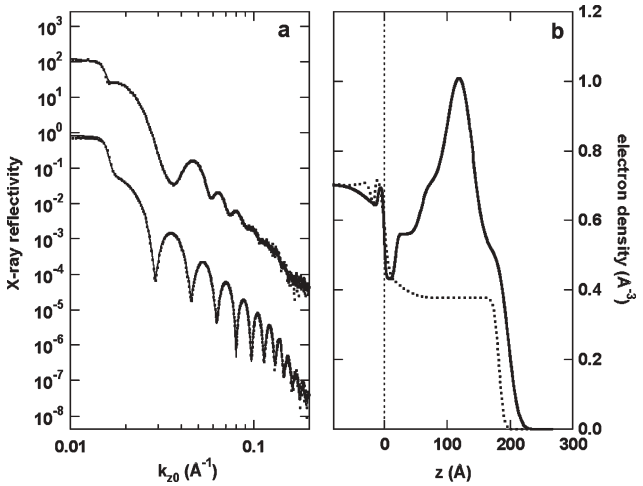

Fig. 5 (a) X-Ray reflectivity plots of the poly-METAC brush before (bottom) and after (top) loading and reduction of $AuCl_4$. The top curve is shifted vertically for clarity. Squares are experimental data and lines are fitted to the data to guide the eye. (b) Electron-density profiles of poly-METAC brushes before (dashed line) and after (continuous line) incorporation and reduction of $AuCl_4$. The Si–brush interface was set to zero vertical distance, and its location is indicated by the vertical dashed line. The perturbation of the electron density in the Si results from plasma cleaning of the Si wafer prior to brush growth. The strong increase in the electron density away from the Si substrate is attributed to the successful incorporation of Au in the polyelectrolyte brush.

For the NP-loaded sample, a sharp increase in the electron density was observed instead, which could be assigned to the presence of the Au NPs. The XRR data provides direct evidence of NP inclusion within the polyelectrolyte brush, rather than on the surface of the organic film. The profiles also indicate that fewer NPs are formed in the brush region close to the Si surface.

The XRR profiles further revealed that the thickness of the poly-METAC-brush layer increased slightly from 17 nm to 19 nm after $AuCl_4$ loading and reduction, whereas the effective electron density of the original poly-METAC brush increased from 65.8 electrons per Å^3 to 129.2 electrons per Å^3 (effective densities were obtained by integrating the electron-density profiles over the entire brush thickness). Nearly 50% of the electron density can be attributed to the Au embedded within the polyelectrolyte brush, corresponding to 63 electrons per square angstrom of brush layer. Using an electron density of 4.67 electrons per Å^3 for Au and 0.38 electrons per Å^3 for the METAC polymer layer based on Fig. 5, we estimate 13 Å^3 of Au and 173 Å^3 of polymer per unit volume ($1 \times 1 \times 190$ Å^3). This corresponds to a volume fraction of 7% Au in the NP-loaded brush, which is in good agreement with the $\sim$10% increase of thickness observed after loading. It should be mentioned that the presence of additional Cl^- ions associated with the partially reduced Au species is not taken into account, resulting in an underestimation of the increase in volume fraction.

In order to evaluate the responsivity of the NP-embedded polyelectrolyte brushes to environmental changes, poly-METAC brushes were prepared on Au substrates in a patterned configuration and loaded with $AuCl_4$, followed by $NaBH_4$ reduction to Au NPs. The latter were expected to produce a sizable plasmon shift upon constriction of the brush layer, which could be studied directly by atomic force microscopy (AFM). Striped polymer brushes (width *ca.* 4 μm) were grown from patterned substrates prepared by micro-contact printing as previously described.[19] This configuration was useful for examining the swelling behavior of the polyelectrolyte-brush layer by AFM, using the polymer-free regions of the substrate for comparing changes in brush height (Fig. 6).

NP-loaded poly-METAC brushes in air (Fig. 6, left) were observed by AFM to be in a fully compressed state, with an average brush height (h) of approximately 25 nm, whereas immersion in water resulted in considerable swelling of the nanocomposite layer ($h \sim 55$ nm). The swelling of the polymer matrix could increase the average interparticle distance between Au NPs embedded within the brush and can be expected to reduce interparticle coupling, causing their plasmon resonances to shift toward higher frequencies. This is in agreement with our results on Au NP-poly-METAC brushes grown on a glass substrate; immersion in water resulted in a blueshift of the absorption maximum by $\sim$18 nm (Fig. 7). It must be noted these changes in the spectra could not be attributed exclusively to interparticle distance. Changes in the refractive index of the particle surrounding the swollen brush (high water content) could also affect the observed shift in the UV-Vis spectra.

Remarkably, the optical response of the NP-loaded poly-METAC brushes remained unchanged after two weeks of storage in water, testifying to the robust quality of the nanocomposite film. The optical absorption of these brushes was also unaffected by a one-week exposure to 0.1 M aqueous NaCl, a condition known to cause considerable shrinkage of the polyelectrolyte brushes.[19,20,33] This implies that the compression of the brush layer was not sufficient to induce a significant electromagnetic coupling between the embedded Au NPs, suggesting their complete encapsulation by the surrounding polyelectrolyte chains.[34,35] Although a thick NP coating limits the range of distances that can be attained through external stimuli, interparticle separations is not the only factor in electromagnetic coupling. For example, it is well known that plasmonic couplings are highly dependent on particle-spacing ratios,[36] so the coupling of larger NPs would produce stronger optical responses.[37] In a similar vein, the plasmon resonances of anisotropic Au NPs (*e.g.* nanorods) are more sensitive than spherical particles to local environmental changes,[38–40] as well as to polarization effects.[41,42] These structural parameters offer additional opportunities for incorporating nanoparticles into stimuli-responsive polyelectrolyte brushes as optically based actuators.

Conclusions

METAC-derived polyelectrolyte brushes can support high loadings of $AuCl_4$ and their *in situ* reduction to Au nanoparticles. These embedded nanoparticles are uniform in size and are fully stabilized by the surrounding polyelectrolyte chains. XRR analysis revealed that the Au NPs are formed within the polymer brush layer, and remained firmly attached after several weeks of storage in aqueous solution. Moreover,

View Article Online

Published on 12 June 2007. Downloaded by Michigan State University on 16/01/2016 02:00:57.

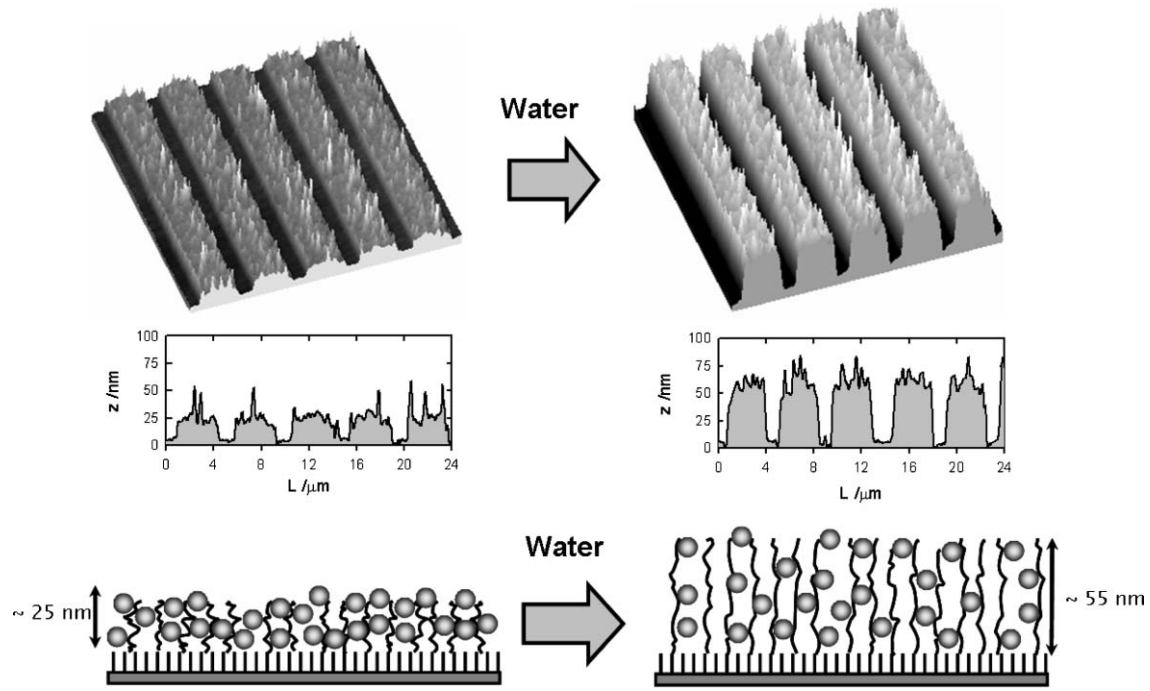

Fig. 6 Patterned poly-METAC brushes loaded with Au NPs, in compressed and swollen states (left and right, respectively). *Top, middle*: AFM images and cross-sectional analyses of patterned brush layers, obtained in air and water; *bottom*: schematic corresponding to AFM data.

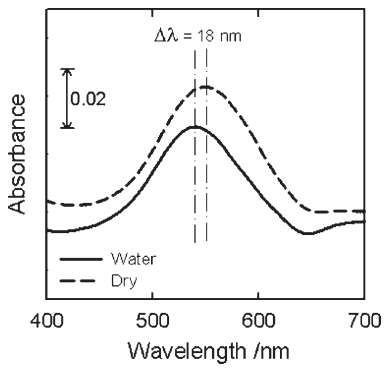

Fig. 7 UV-Vis absorption spectra of "dry" Au NP-loaded poly-METAC brushes in air (dashed line), and the same brushes immersed in water (solid line). Polyelectrolyte brushes were grown on glass substrates.

AFM experiments showed that the swelling behaviour of the brush layer is not perturbed by the presence of the loaded NPs. The Au NP-poly-METAC nanocomposite is remarkably stable to aqueous environments, suggesting the feasibility of producing actuators based on nanoparticles embedded within stimuli-responsive polymer-brush layers.

Acknowledgements

O. A. acknowledges a Marie Curie Research Fellowship. A. M. J. acknowledges financial support from the Leverhulme Trust (visiting professorship). A. W. thanks the Department of Materials Science and Metallurgy (University of Cambridge) for the use of their electron microscopy facilities during a sabbatical leave from Purdue University.

References

1 J. S. Bradley, in *Clusters and Colloids: From Theory to Applications*, ed. G. Schmid, VCH-Wiley, Wienheim, 1994, ch. 6, pp. 459–544.
2 Y. Yamanoi, N. Shirahata, T. Yonezawa, N. Terasaki, N. Yamamoto, Y. Matsui, K. Nishio, H. Masuda, Y. Ikuhara and H. Nishihara, *Chem.–Eur. J.*, 2006, **12**, 314–323.
3 R. Bhat, J. Genzer, B. N. Chaney, H. W. Sugg and A. Liebmann-Vinson, *Nanotechnology*, 2003, **14**, 1145–1152.
4 S. Kidambi and M. L. Bruening, *Chem. Mater.*, 2005, **17**, 301–307.
5 F.-K. Liu, S.-Y. Hsieh, F.-H. Ko, T.-C. Chu and B.-T. Dai, *Jpn. J. Appl. Phys., Part 1*, 2003, **43**, 4147–4151.
6 R. Shenhar, T. B. Norsten and V. M. Rotello, *Adv. Mater.*, 2005, **17**, 657–669.
7 M. Kuang, D. Wang and H. Möhwald, *Adv. Funct. Mater.*, 2005, **15**, 1611–1616.
8 V. Pardo-Yissar, R. Gabai, A. N. Shipway, T. Bourenko and I. Willner, *Adv. Mater.*, 2001, **13**, 1320–1323.
9 I. Tokareva, S. Minko, J. H. Fendler and E. Hutter, *J. Am. Chem. Soc.*, 2004, **126**, 15950–15951.
10 T. C. Wang, M. F. Rubner and R. E. Cohen, *Langmuir*, 2002, **18**, 3370–3375.
11 L. Sun and R. M. Crooks, *Langmuir*, 2002, **18**, 8231–8236.
12 S. Joly, R. Kane, L. Radzilowski, T. Wang, A. Wu, R. E. Cohen, E. L. Thomas and M. F. Rubner, *Langmuir*, 2000, **16**, 1354–1359.
13 S. Dante, Z. Hou, S. Risbud and P. Stroeve, *Langmuir*, 1999, **15**, 2176–2182.
14 K. S. Mayya, B. Schoeler and F. Caruso, *Adv. Funct. Mater.*, 2003, **13**, 183–187.
15 S. G. Boyes, B. Akgun, W. J. Brittain and M. D. Foster, *Macromolecules*, 2003, **36**, 9539–9548.
16 M. Husseman, E. E. Malmstrom, M. McNamara, M. Mate, D. Mecerreyes, D. G. Benoit, J. L. Hedrick, P. Mansky, E. Huang, T. P. Russell and C. J. Hawker, *Macromolecules*, 1999, **32**, 1424–1431.
17 V. L. Osborne, D. M. Jones and W. T. S. Huck, *Chem. Commun.*, 2002, 1838–1839.
18 S. E. Moya, A. A. Brown, O. Azzaroni and W. T. S. Huck, *Macromol. Rapid Commun.*, 2005, **26**, 1117–1121.
19 O. Azzaroni, S. E. Moya, T. Farhan, A. A. Brown and W. T. S. Huck, *Macromolecules*, 2005, **38**, 10192–10199.

 This journal is © The Royal Society of Chemistry 2007

View Article Online

20 S. E. Moya, O. Azzaroni, T. Farhan, V. L. Osborne and W. T. S. Huck, *Angew. Chem., Int. Ed.*, 2005, **44**, 4578–4581.
21 Y. Marcus, *Ion Solvation*, John Wiley & Sons, Chichester, 1985.
22 K. Esumi and K. Torigoe, *Langmuir*, 1992, **8**, 59–63.
23 O. Azzaroni, S. E. Moya, A. A. Brown, Z. Zheng, E. Donath and W. T. S. Huck, *Adv. Funct. Mater.*, 2006, **16**, 1037–1042.
24 O. Azzaroni, Z. Zheng, Z. Yang and W. T. S. Huck, *Langmuir*, 2006, **26**, 6730–6733.
25 S. Praharaj, S. Nath, S. K. Ghosh, S. Kundu and T. Pal, *Langmuir*, 2004, **20**, 9889–9892.
26 E. R. Els, L. Lorenzen and C. Aldrich, *Miner. Eng.*, 2000, **13**, 401–413.
27 G. Sharma and M. Ballauff, *Macromol. Rapid Commun.*, 2004, **25**, 547–552.
28 M. Brust, M. Walker, D. Bethell, D. J. Schiffrin and R. Whyman, *J. Chem. Soc., Chem. Commun.*, 1994, 801–802.
29 M.-C. Daniel and D. Astruc, *Chem. Rev.*, 2004, **104**, 293–346.
30 U. Kreibig and M. Vollmer, *Optical Properties of Metal Clusters*, Springer, New York, 1995, vol. 25.
31 J. J. Storhoff, A. A. Lazarides, R. C. Mucic, C. A. Mirkin, R. L. Letsinger and G. C.Schatz, *J. Am. Chem. Soc.*, 2000, **122**, 4640–4650.
32 B. Kim, S. L. Tripp and A. Wei, *J. Am. Chem. Soc.*, 2001, **123**, 7955–7956.
33 M. Biesalski, D. Johannsmann and J. Rühe, *J. Chem. Phys.*, 2004, **120**, 8807–8814.
34 A. B. R. Mayer and J. E. Mark, *J. Macromol. Sci., Pure Appl. Chem.*, 1997, **A31**, 2151–2164.
35 Y. Liu, Y. Wang and R. O. Claus, *Chem. Phys. Lett.*, 1998, **298**, 315.
36 D. A. Genov, A. K. Sarychev, V. M. Shalaev and A. Wei, *Nano Lett.*, 2004, **4**, 153–158.
37 R. A. Reynolds, C. A. Mirkin and R. L. Letsinger, *J. Am. Chem. Soc.*, 2000, **122**, 3795–3796.
38 S. Link, M. B. Mohamed and M. A. El-Sayed, *J. Phys. Chem. B*, 1999, **103**, 3073–3077.
39 A. D. McFarland and R. P. van Duyne, *Nano Lett.*, 2003, **3**, 1057–1062.
40 D. A. Zweifel and A. Wei, *Chem. Mater.*, 2005, **17**, 4256–4261.
41 K. Imura, T. Nagahara and H. Okamoto, *J. Phys. Chem. B*, 2005, **109**, 13214–13220.
42 H. Wang, T. B. Huff, D. A. Zweifel, W. He, P. S. Low, A. Wei and J.-X. Cheng, *Proc. Natl. Acad. Sci. U. S. A.*, 2005, **102**, 15752–15756.

Published on 12 June 2007. Downloaded by Michigan State University on 16/01/2016 02:00:57.

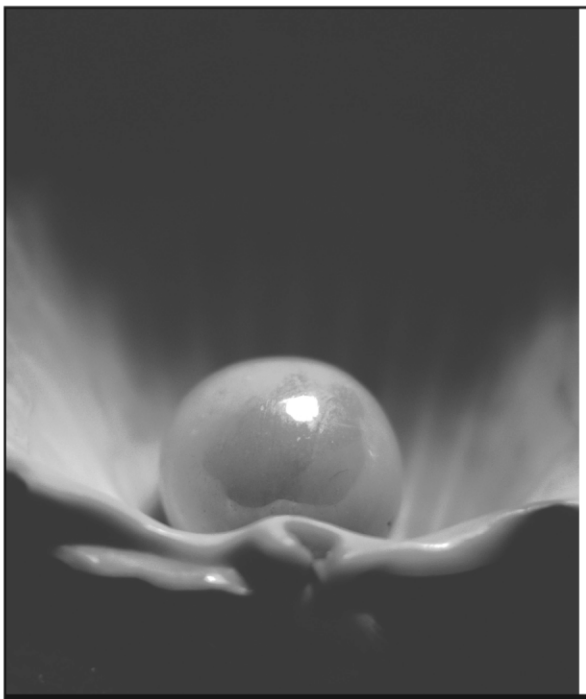

Looking for that **special** research paper from applied and technological aspects of the chemical sciences?

TRY this free news service:

Chemical Technology

- highlights of newsworthy and significant advances in chemical technology from across RSC journals
- free online access
- updated daily
- free access to the original research paper from every online article
- also available as a free print supplement in selected RSC journals.*

*A separately issued print subscription is also available.

Registered Charity Number: 207890

2203683

RSC Publishing

www.rsc.org/chemicaltechnology